GSK2795039 Prevents Tumor Necrosis Factor-α-Induced RIP1-RIP3-MLKL-Mediated Necroptosis in H9C2 Cardiomyocytes Through Inhibition of NADPH Oxidase

Li-Guo YANG[1,2,3]*, Ai-Ling WANG[1,3]*, Run-Nan TANTAI[1,3], Bin YANG[1,3], Yan LIU[2], Chen-Mo-Zhen LI[1,3], Yi LIU[1,3], Rong-Shu LING[1,3], Bao LI[1,3], Fu-Zhong QIN[1,3], Jia-Pu WANG[3,4]

** These authors contributed equally to this work.*

[1]The Second Hospital of Shanxi Medical University, Taiyuan, Shanxi, P. R. China, [2]Shanxi Provincial People's Hospital, Taiyuan, Shanxi, P. R. China, [3]Shanxi Medical University, Taiyuan 030001, Shanxi, P. R. China, [4]Shanxi Provincial Cardiovascular Hospital, Taiyuan, Shanxi, P. R. China

Received March 12, 2026
Accepted July 21, 2026

Summary

Inflammatory cytokines and oxidative stress contribute to heart failure. Tumor necrosis factor-α (TNF-α), a major inflammatory cytokine, induces reactive oxygen species (ROS) and necroptosis in cardiomyocytes. GSK2795039 is a novel NADPH oxidase 2 inhibitor. However, it is unknown whether GSK2795039 prevents TNF-α-induced cardiomyocyte necroptosis and the underlying mechanisms. In the present study, we tested the hypothesis that GSK2795039 prevents TNF-α-induced necroptosis in cardiomyocytes through inhibition of NADPH oxidase-mediated RIP1-RIP3-MLKL pathway. The H9C2 cardiomyocytes were divided into the following groups: control, necrostatin-1, TNF-α, and TNF-α plus necrostatin-1; control, GSK2795039, TNF-α, and TNF-α plus GSK2795039. ROS were assessed by dihydroethidium staining. Necroptotic and apoptotic proteins were measured by Western blot. The RIP1 inhibitor necrostatin-1 attenuated apoptosis, necrosis, phosphorylated RIP3 (p-RIP3) and p-MLKL protein and intracellular ROS in TNF-α-treated H9C2 cardiomyocytes. GSK2795039 inhibited TNF-α-induced Nox2 expression, intracellular ROS and cell death. GSK2795039 prevented the increases in phosphorylated RIP1 (p-RIP1), p-RIP3 and p-MLKL proteins, reflective of their respective kinase activities, markers of necroptosis, in TNF-α-treated H9C2 cardiomyocytes. GSK2795039 prevented the decrease in anti-apoptotic Bcl-2 protein and the increases in pro-apoptotic Bax protein, phosphorylated JNK protein and cleaved caspase 3 protein, indicative of caspase activity, a marker of apoptosis, in TNF-α-treated H9C2 cardiomyocytes. The results indicate that GSK2795039 prevented TNF-α-induced RIP1-RIP3-MLKL-mediated necroptosis in H9C2 cardiomyocytes through inhibition of NADPH oxidase-derived ROS. These findings advocate for further animal testing of the specific Nox2 inhibitor GSK2795039 in myocardial infarction and heart failure, which are characterized by elevated levels of inflammatory cytokines such as TNF-α and oxidative stress.

Key words

Tumor necrosis factor-α • Inflammatory cytokines • Reactive oxygen species • Necroptosis • Cardiomyocytes

Corresponding author

F.-Z. Qin, The Second Hospital of Shanxi Medical University, 382 Wuyi Road, Taiyuan 030001, Shanxi, P. R. China. E-mail: sxcvh13@sina.com

Introduction

Inflammation is a key contributor in the pathophysiology of cardiovascular diseases [1,2]. Numerous studies have shown that the levels of inflammatory cytokines, including tumor necrosis factor-α (TNF-α), interleukin (IL)-1, and IL-6 are increased in myocardial infarction and heart failure [1,3,4]. TNF-α is the most studied one in heart failure. Both basic and clinical

 An open access article under the CC BY 4.0 license https://creativecommons.org/licenses/by/4.0/ © 2026 by the authors. Published by the Institute of Physiology, Czech Academy of Sciences, Prague, Czech Republic. E-mail: physres@fgu.cas.cz, www.biomed.cas.cz/physiolres

studies indicate that there is a direct relationship between the level of TNF and the severity of heart failure [5,6]. Transgenic mice with cardiac specific overexpression of TNF-α exhibit dilated cardiomyopathy [7]. However, the cellular and molecular mechanism that TNF-α mediates cardiac remodeling and failure has not been fully understood. Evidence has accumulated that in cardiac myocytes *in vitro* TNF-α induces hypertrophy and apoptosis, both of which contribute to myocardial remodeling and failure [8,9].

Necroptosis (programmed necrosis), a newly discovered form of cell death, is mediated by a complex set of proteins involving receptor-interacting protein kinase 1 and 3 (RIP1, RIP3) and mixed lineage kinase domain-like protein (MLKL) [10,11]. Studies have recently shown that TNF-α induces necroptosis in cultured cardiomyocytes [12,13]. However, the mechanism of TNF-α-induced cardiomyocyte necroptosis remains to be elucidated. TNF-α has been shown to induce reactive oxygen species (ROS) in cardiomyocytes [14]. NADPH oxidase is a main source of ROS and Nox2 is a major subunit of NADPH oxidase [15,16]. TNF-α mediates NADPH oxidase activation and ROS in cardiomyocytes [17].

GSK2795039 is a novel small molecular NADPH oxidase 2 (Nox2) inhibitor [18,19]. Our recent studies have shown that the specific Nox2 inhibitor GSK2795039 prevents myocyte necroptosis in doxorubicin-induced heart failure [20], which is characterized by increased TNF-α [21]. However, it is unknown whether the specific Nox2 inhibitor GSK2795039 prevents TNF-α-induced myocyte necroptosis and the underlying mechanisms. In the present study, we tested the hypothesis that GSK2795039 prevents TNF-α-induced necroptosis in cardiomyocytes through inhibition of NADPH oxidase-mediated RIP1-RIP3-MLKL signaling pathway.

Materials and Methods

H9C2 cardiomyocyte culture and treatments

The H9C2 rat cardiomyocyte line was purchased from the Cell Bank of Chinese Academy of Sciences (American Type Culture Collection, ATCC, Cat# CRL-1446, RRID:CVCL_0286). The H9C2 cardiomyocytes were cultured in Dulbecco's modified Earle's medium (DMEM) (Gibco, Life Technologies, USA, Cat# 11995065) with 3.7 g/l sodium bicarbonate, 4.5 g/l D-glucose, and 110 mg/l sodium pyruvate, supplemented with 10 % fetal bovine serum (Gibco, Life Technologies, Cat# 10099141) and penicillin (100 units/ml) and streptomycin (100 μg/ml) in a humidified incubator with 95 % air and 5 % CO_2 at 37 °C. The culture medium was changed every two days. After four days, cells were passaged at a 1:6 ratio and seeded at the density of 0.15×10^6 cells per 35-mm well of six-well plates. These cells were cultured for three days and then performed treatments as we have described [20,22].

We first determined the effect of necrostatin-1 (Nec-1), a RIP1-targeted inhibitor of necroptosis in H9C2 cardiomyocytes after exposure to TNF-α. The H9C2 cardiomyocytes were divided into four experimental groups as follow: (1) control group (normal DMEM), (2) Nec-1 group (Cayman Chemical, Ann Arbor, Michigan, USA. Cat#: 11658) (20 μM), (3) TNF-α group (TNF-α, Millipore Sigma, Burlington, MA, USA. Cat#: T5944) (50 ng/ml), (4) TNF-α plus Nec-1 group, the cells were pretreated with 20 μM Nec-1 30 min before TNF-α treatment. The doses of TNF-α and Nec-1 were based on our pilot study and the previous reports [23-25]. The H9C2 cells were treated for 24 h and then the cell lysates were collected for the assays.

Second, we investigated the effects of GSK2795039 on ROS, necroptosis and apoptosis in H9C2 cardiomyocytes after exposure to TNF-α. The H9C2 cardiomyocytes were divided into four experimental groups as follow: (1) control group (normal DMEM), (2) GSK2795039 group (GSK, MedChemExpress, Monmouth Junction, NJ, USA. Cat#: HY-18950) (25 μM), (3) TNF-α group (TNF-α, Millipore Sigma) (50 ng/ml), (4) TNF-α plus GSK group, the cells were pretreated with 25 μM GSK 30 min before TNF-α treatment. The doses of TNF-α and GSK and the incubation time were based on our pilot study and the previous reports [20,23,24]. The H9C2 cells were treated for 24 h and then the cell lysates were collected for the assays.

Detection of reactive oxygen species production

H9C2 cardiomyocytes at 24 h after co-treatment of TNF-α and Nec-1 or GSK were washed with PBS and then incubated with dihydroethidium (DHE, 10 μmol/l; Thermo Fisher Scientific, Waltham, MA, USA. Cat#: D-1168) at a cell incubator for 30 min as we have described previously [26]. The cells were washed with PBS and then mounted with antifade medium (Vector Laboratory, Burlingame, CA). The slides were examined under a confocal laser scanning microscopy (FV3000, Olympus, Japan).

Flow cytometry

Cardiomyocyte apoptosis and necrosis were detected using an Annexin V: FITC Apoptosis Detection Kit I (BD Pharmingen, San Diego, CA, USA) according to the manufacturer's instructions and our previous report [20]. Briefly, the cells were washed with PBS, resuspended in the binding buffer and incubated with Annexin V-FITC and propidium iodide (PI) solution. The samples were analyzed using flow cytometry (Beckman Coulter, Miami, FL, USA). Apoptotic cells, which stained positive for Annexin V-FITC and negative or positive for PI, necrotic cells, which stained only positive for PI (negative for annexin V-FITC), and living cells, which stained negative for both Annexin V-FITC and PI were counted and represented as a percentage of the total cell count.

Immunofluorescence for Nox2 expression

H9C2 cells were fixed in 4 % paraformaldehyde in phosphate-buffered saline (PBS), incubated in 0.1 %Triton X-100 in PBS, washed in PBS, blocked with 5 % bovine serum albumin, and subsequently incubated with primary antibody mouse anti-Nox2 (gp91phox) IgG (catalog number: sc-74514, Santa Cruz Biotechnology, Santa Cruz, CA), and then incubated with secondary antibody goat anti-mouse IgG conjugated FITC (catalog number: sc-2010, Santa Cruz Biotechnology). The cells were washed in PBS, incubated with 4',6-diamidino-2-phenylindole (DAPI, catalog number: AR1176, BOSTER, China) and then mounted with antifade medium (Vector Laboratory, Burlingame, CA). The samples were examined under a confocal laser scanning microscope (FV3000, Olympus, Japan).

Western blot

H9C2 cells were homogenized in a RIPA lysis buffer (Boster Biological Technology, Wuhan, Hubei, China) as we have described [20]. Protein extracts were resolved by electrophoresis in 8-12 % sodium dodecyl-sulfate-polyacrylamide gel and transferred to polyvinyl-lidene fluoride membranes. The membranes were blocked in 5 % bovine serum albumin or 5 % nonfat dry milk in Tris-buffered saline containing 0.05 % Tween 20 (TBST). The resulting blots were incubated at 4 °C overnight with primary antibodies: rabbit monoclonal anti-RIP1 antibody (Cell Signaling Technology Cat# 3493, RRID:AB_2305314), rabbit monoclonal anti-phospho-RIP1 antibody (Cell Signaling Technology Cat# 53286, RRID:AB_2925183), mouse monoclonal anti-RIP3 antibody (Santa Cruz Biotechnology Cat# sc-374639, RRID:AB_10992232), rabbit monoclonal anti-phospho-RIP3 antibody (Abcam Cat# ab209384, RRID:AB_2714035), rat monoclonal anti-MLKL antibody (Abcam Cat# ab243142), rabbit polyclonal anti-phospho-MLKL antibody (Thermo Fisher Scientific Cat# PA5-105678, RRID:AB_281710), mouse monoclonal anti-Bcl-2 antibody (Santa Cruz Biotechnology, Cat# sc-7382), mouse monoclonal anti-Bax antibody (Santa Cruz Biotechnology, Cat# sc-7480), rabbit polyclonal anti-caspase 3 antibody (Santa Cruz Biotechnology, Cat# sc-373730), rabbit polyclonal anti-cleaved caspase 3 antibody (Cell Signaling Technology, Cat# 9664,), mouse monoclonal anti-GAPDH antibody (Abcam, Cat# ab8245, RRID:AB_2107448) and mouse monoclonal anti-β-actin antibody (Santa Cruz Biotechnology, Cat# sc-47778, RRID:AB_62663). After the incubation of primary antibodies, blots were incubated with the secondary antibody goat anti-mouse IgG-HRP (Abcam), goat anti-rat IgG-HRP (Abcam) or goat anti-rabbit IgG-HRP (Abcam). The membrane was washed with TBST and then the bands were visualized with an Ultra High Sensitivity ECL kit (Thermo Scientific Pierce, Waltham, MA) and the Gel Imaging System (Bio-Rad, CA) and quantified using Labwork4.6 image analysis software. The optical density of samples was normalized to a control sample in an arbitrary densitometry unit.

Statistical analysis

The data were analyzed with GraphPad Prism 5 software (GraphPad Software, Inc. La Jolla, CA, USA). Results are presented as means ± standard deviation of the mean (S.D.). The statistical significance of differences among groups was determined using one-way analysis of variance (ANOVA) and Bonferroni's or Newman-Keuls multiple Comparison Tests. A value of $P<0.05$ was considered statistically significant.

Results

Effects of Nec-1 on necroptosis and intracellular ROS in TNF-α-treated H9C2 cardiomyocytes

Flow cytometry analysis showed that the rates of apoptosis and necrosis were increased in H9C2 cardio-myocytes after exposure to TNF-α (Fig. 1A-C). These alterations were prevented by the treatment of Nec-1, a RIP1 inhibitor (Fig. 1A-C). Western blot showed that RIP3 and MLKL protein expression had no change

(Fig. 1D and F) (Fig. 2A, C), but phosphorylated protein of RIP3 (p-RIP3) and p-MLKL, markers of necroptosis, were markedly increased in H9C2 cardiomyocytes after exposure to TNF-α and the increases were prevented by the treatment of the RIP1 inhibitor Nec-1 (Fig. 1E and G) (Fig. 2B and D). These findings confirm that TNF-α induces necroptosis in H9C2 cardiomyocytes. In addition, we found that intracellular ROS (O_2^- in particular) production assessed by DHE [26] was increased in H9C2 cardiomyocytes after exposure to TNF-α and Nec-1 treatment attenuated the increase in ROS induced by TNF-α (Fig. 2E, F).

Effects of GSK2795039 on Nox2 expression and intracellular ROS in TNF-α-treated H9C2 cardiomyocytes

In TNF-α-treated H9C2 cardiomyocytes, Nox2 protein expression assessed by immunofluorescence was markedly increased and the increase was prevented by the treatment of GSK2795039 (Fig. 2G, H). Intracellular ROS (O_2^- in particular) production was increased in H9C2 cardiomyocytes after exposure to TNF-α and GSK2795039 treatment attenuated the increase in ROS induced by TNF-α (Fig. 3A, B). These results suggest that GSK2795039 inhibits Nox2 protein expression and prevents intracellular ROS productions in TNF-α-treated H9C2 cardiomyocytes.

Effects of the Nox2 inhibitor GSK2795039 on TNF-α-induced H9C2 cardiomyocyte death

Cardiomyocyte death was assessed by an Annexin V-FITC Apoptosis Detection Kit using flow cytometry as we have described [20]. In TNF-α-treated H9C2 cardiomyocytes, the rates of necrosis and apoptosis were increased, and GSK2795039 attenuated the increases in TNF-α-treated cells (Fig. 3C-E). The data suggest that the Nox2 inhibitor GSK2795039 prevents TNF-α-induced H9C2 cardiomyocyte death.

Effects of the Nox2 inhibitor GSK2795039 on TNF-α-induced necroptosis in H9C2 cardiomyocytes

To assess the effects of the Nox2 inhibitor GSK2795039 on cardiomyocyte necroptosis, we analyzed RIP1, RIP3 and MLKL protein expression and phosphorylated protein expression of RIP1, RIP3 and MLKL, indicative of their respective activities, markers of necroptosis [11,27], by Western blot. In TNF-α-treated cells, RIP1 protein expression was decreased and phosphorylated protein expression of RIP1 (p-RIP1) was increased, and the Nox2 inhibitor GSK2795039 treatment had no effect on RIP1 protein expression but prevented the increase in p-RIP1 protein expression (Fig. 4A-D). In TNF-α-treated H9C2 cardiomyocytes, RIP3 and MLKL protein expression had no change, but phosphorylated protein of RIP3 (p-RIP3) and phosphorylated protein of MLKL (p-MLKL) were markedly increased and the increases were prevented by the treatment of GSK2795039 (Fig. 4E-L). These results indicate that the Nox2 inhibitor GSK2795039 prevents RIP-RIP3-MLKL mediated necroptosis in TNF-α-treated H9C2 cardiomyocytes. These findings suggest NAPDH oxidase-derived ROS mediate TNF-α-induced cardiomyocyte necroptosis.

Effects of GSK2795039 on TNF-α-induced apoptosis in H9C2 cardiomyocytes

Consistent with previous reports [28], we have shown that in TNF-α-treated H9C2 cardiomyocytes, anti-apoptotic protein Bcl-2 was decreased, proapoptotic protein Bax was increased, the ratio of Bcl-2/Bax was decreased, JNK and phosphorylated JNK proteins were increased and the changes were prevented by the treatment of the Nox2 inhibitor GSK2795039 (Fig. 5A-I). In TNF-α-treated H9C2 cardiomyocytes, total caspase 3 protein had no change, but cleaved caspase 3 protein, indicative of caspase activity, a marker of apoptosis, was markedly increased (Fig. 6A-D). GSK2795039 treatment prevented the increase in cleaved caspase 3 protein in TNF-α-treated H9C2 cardiomyocytes (Fig. 6A-D). These findings suggest that the Nox2 inhibitor GSK2795039 prevents apoptosis in TNF-α-treated H9C2 cardiomyocytes through JNK/Bcl-2/Bax signaling pathway.

Discussion

The main goal of this study was to assess the effects of the specific Nox2 inhibitor GSK2795039 on TNF-α-induced necroptosis in H9C2 cardiomyocytes and the underlying mechanisms. Our results indicate that GSK2795039 prevents TNF-α-induced RIP1-RIP3-MLKL-mediated necroptosis in H9C2 cardiomyocytes through inhibition of NADPH oxidase-derived ROS. These findings advocate for further animal testing of the specific Nox2 inhibitor GSK2795039 in acute myocardial ischemia and reperfusion and heart failure, which are characterized by elevated levels of inflammatory cytokines such as TNF-α and oxidative stress [3,6,29].

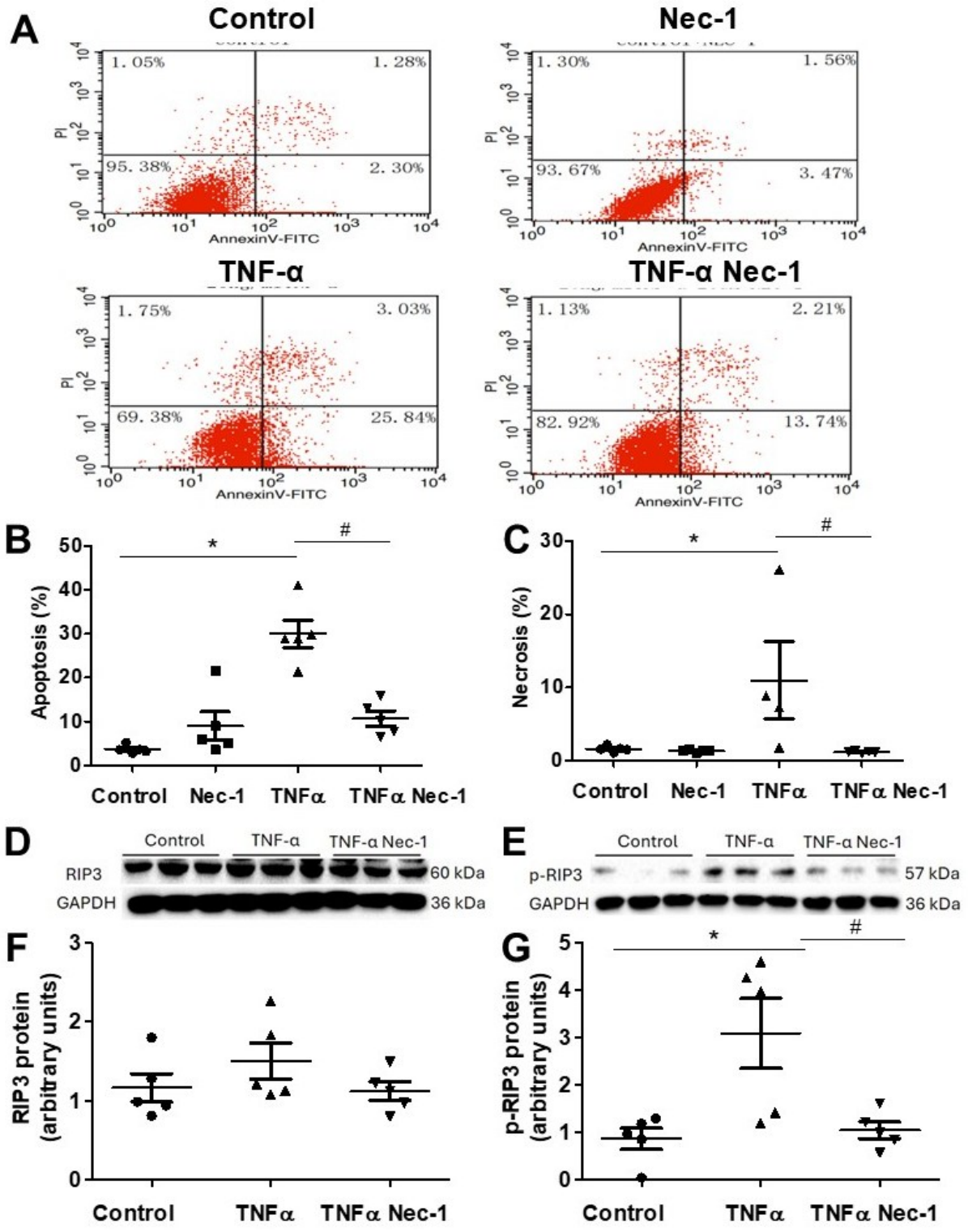


Fig. 1. Effect of the RIP1 inhibitor necrostatin-1 (Nec-1) on apoptosis, necrosis and necroptosis in H9C2 cardiomyocytes after exposure to tumor necrosis factor-α (TNF-α). (**A-C**) Apoptosis and necrosis using flow cytometry analysis. (**D** and **E**) Representative Western blots of RIP3 and p-RIP3. Equal loading of proteins is illustrated by GAPDH bands. (**F** and **G**) The graphs show the relative expression of RIP3 and p-RIP3 proteins in the three groups, respectively. Values are means ± S.D.; n=5 for B. n=4-5 for C. n=5 for F and G. * P<0.05 vs. Control or Nec-1 group; # P<0.05 vs. TNF-α group.

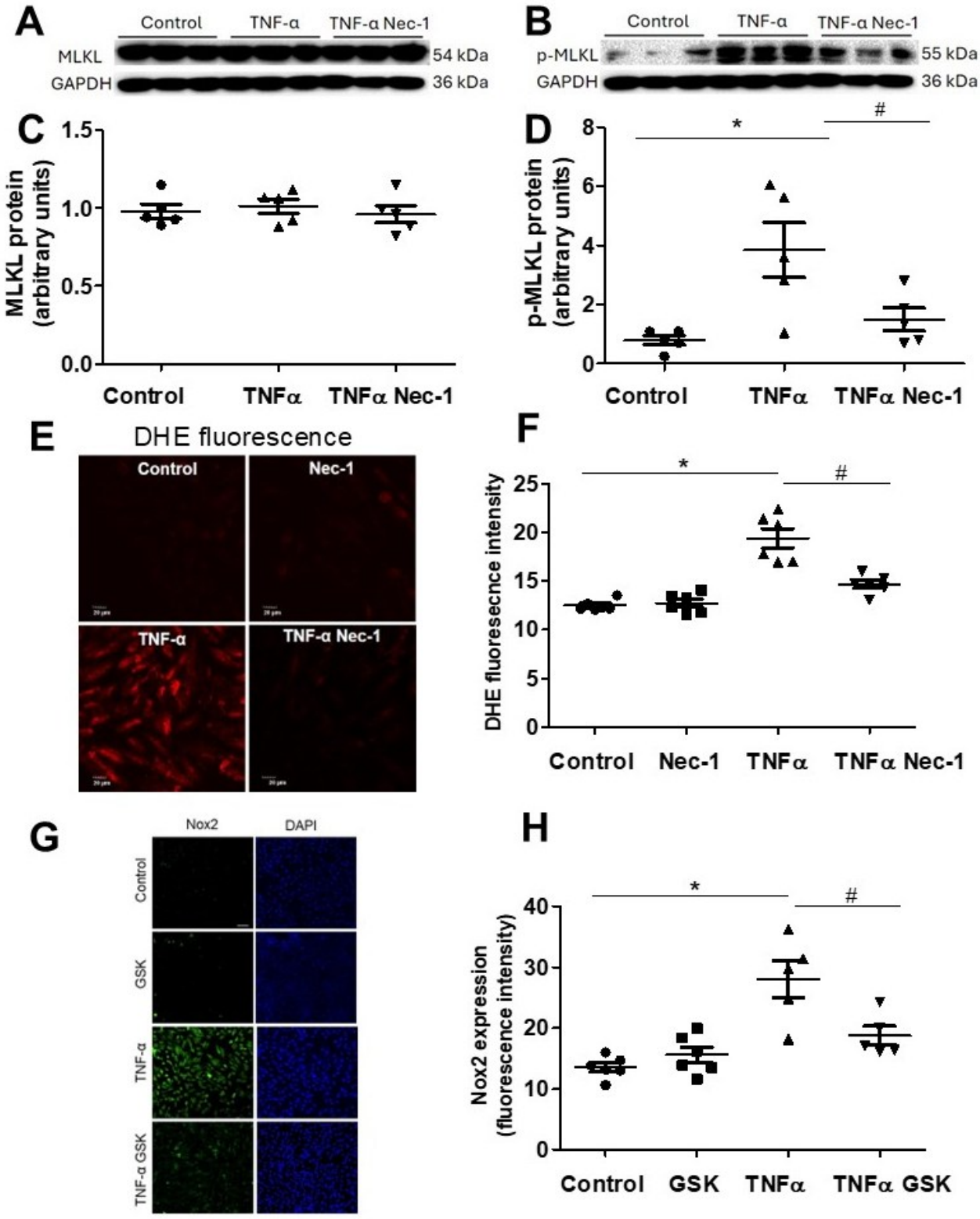


Fig. 2. (**A** and **B**) Representative Western blots of MLKL and p-MLKL. Equal loading of proteins is illustrated by GAPDH bands. (**C** and **D**) The graphs show the relative expression of MLKL and p-MLKL proteins in the three groups, respectively. Values are means ± S.D.; n=5 for **C** and **D**. * P<0.05 vs. Control group; # P<0.05 vs. TNF-α group. (**E** and **F**). Effect of the RIP1 inhibitor necrostatin-1 (Nec-1) on intracellular reactive oxygen species (ROS) in H9C2 cardiomyocytes after exposure to tumor necrosis factor-α (TNF-α). (**E**) Representative photomicrographs of H9C2 cardiomyocytes stained by dihydroethidium (DHE). DHE staining is shown by red fluorescence. Bar=20 μm. (**F**). The relative fluorescence intensity of DHE measured by ImageJ. Values are means ± S.D.; n=6. * P<0.05 vs. Control or Nec-1 group; # P<0.05 vs. TNF-α group. (**G** and **H**) GSK2795039 (GSK) attenuates NADPH oxidase 2 (Nox2) protein expression in H9C2 cardiomyocytes after exposure to TNF-α. (**G**) Immunofluorescence for Nox2. Nox2 staining is shown by green fluorescence. Nuclei shown by blue fluorescence. Bar = 100 μm. (**H**) Fluorescence intensity of Nox2 measured by ImageJ. Values are means ± S.D.; n=5-6. * P<0.05 vs. Control or GSK group; # P<0.05 vs. TNF-α group.

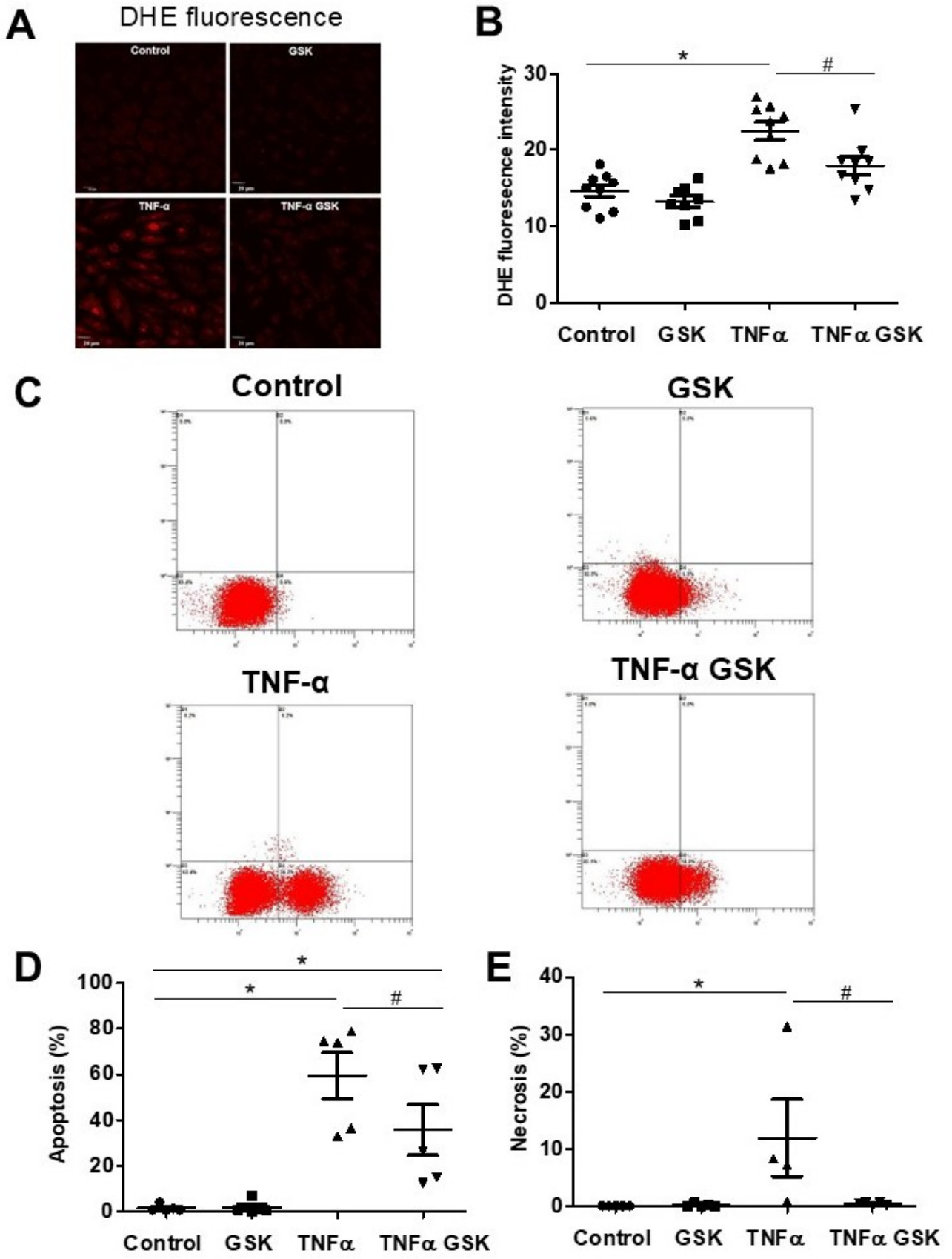


Fig. 3. Effect of the Nox2 inhibitor GSK2795039 (GSK) on intracellular ROS, apoptosis and necrosis in H9C2 cardiomyocytes after exposure to tumor necrosis factor-α (TNF-α). (**A**) Representative photomicrographs of H9C2 cardiomyocytes stained by DHE. DHE staining is shown by red fluorescence. Bar=20 μm. (**B**) The relative fluorescence intensity of DHE measured by ImageJ. Values are means ± S.D.; n = 8-9. * P<0.05 vs. Control or GSK group; # P<0.05 vs. TNF-α group. (**C-E**) Apoptosis and necrosis using flow cytometry analysis. Values are means ± S.D.; n=5. * P<0.05 vs. Control or GSK group; # P<0.05 vs. TNF-α group.

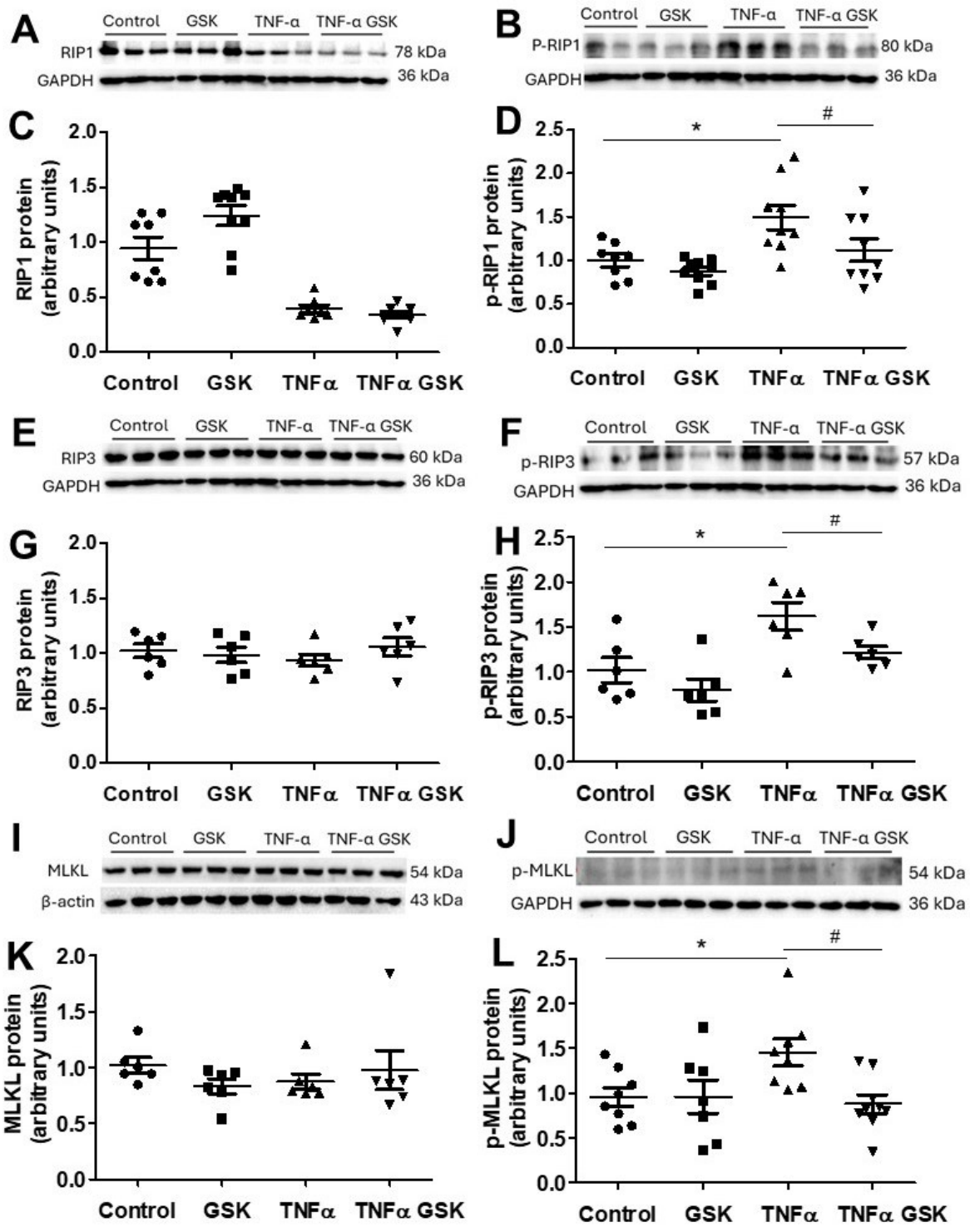


Fig. 4. The Nox2 inhibitor GSK2795039 (GSK) prevents necroptosis in H9C2 cardiomyocytes after exposure to tumor necrosis factor-α (TNF-α). (**A, B, E, F, I** and **J**) Representative Western blots of RIP1, phosphorylated RIP1 (p-RIP1), RIP3, phosphorylated RIP3 (p-RIP3), MLKL and phosphorylated MLKL (p-MLKL) proteins, respectively. Equal loading of proteins is illustrated by GAPDH or β-actin bands. (**C, D, G, H, K** and **L**) The graphs show the relative expression of RIP1, p-RIP1, RIP3, p-RIP3, MLKL and p-MLKL proteins in the four groups, respectively. Values are means ± S.D.; n=7-9 for A. n=8-9 for B. n=6 for G, H and K. n=7-9 for L. * $P<0.05$ vs. Control or GSK group; # $P<0.05$ vs. TNF-α group.

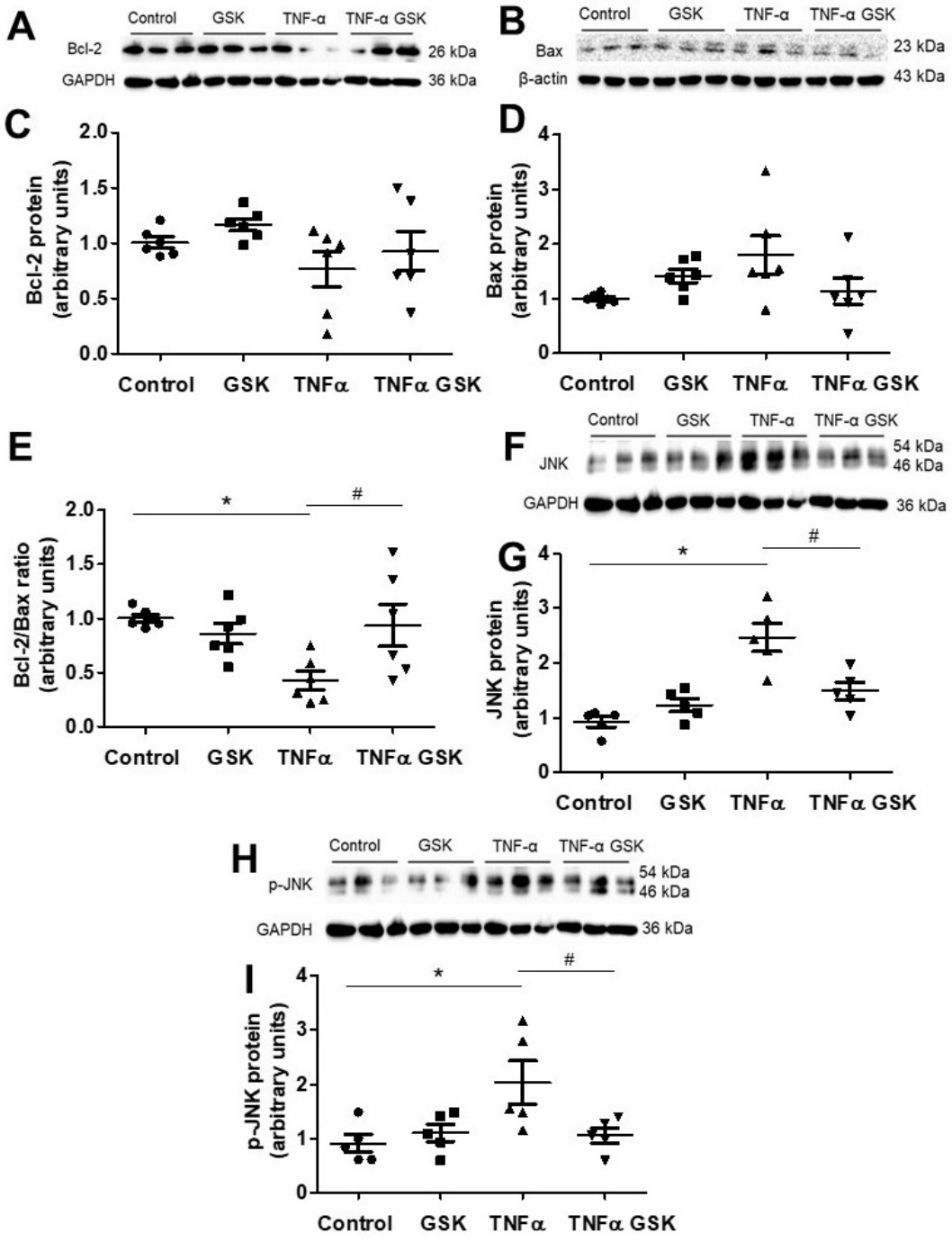


Fig. 5. Effect of the Nox2 inhibitor GSK2795039 (GSK) on Bcl-2, Bax, JNK and phosphorylated JNK (p-JNK) protein expression in H9C2 cardiomyocytes after exposure to tumor necrosis factor-α (TNF-α). (**A, B, F** and **H**) Representative Western blots of Bcl-2, Bax, JNK and phosphorylated JNK (p-JNK) proteins, respectively. Equal loading of proteins is illustrated by GAPDH or β-actin bands. (**C, D, G** and **I**) The graphs show the relative expression of Bcl-2, Bax, JNK and p-JNK proteins in the four groups, respectively. (**E**) The graph shows the ratio of Bcl2/Bax. Values are means ± S.D.; n=6 for C, D and E. n=5 for G and I. * P<0.05 vs. Control or GSK group; # P<0.05 vs. TNF-α group.

Nec-1 prevents TNF-α-induced necroptosis and apoptosis in H9C2 cardiomyocytes

We and others have recently demonstrated that myocyte necroptosis (programmed necrosis) is increased in myocardial infarction, pressure overload-induced heart failure and doxorubicin-induced cardiomyopathy [20,30,31]. Increased myocyte necroptosis contributes to myocardial remodeling and heart failure [3,6]. Studies have shown that the interplay of TNF-α and ROS is related to cardiomyocyte necroptosis [4,14,30]. Our present study has demonstrated that Nec-1, a RIP1 inhibitor, inhibited necroptosis in TNF-α-treated H9C2 cardiomyocytes,

indicating that TNF-α induces cardiomyocyte necroptosis. We have further found that the RIP1 inhibitor Nec-1 inhibited TNF-α-induced cardiomyocyte apoptosis. The mechanism that Nec-1 inhibits apoptosis remains unclear, but it might be related to the indirect effects of Nec-1 on ROS. The present study confirmed that the RIP1 inhibitor Nec-1 prevented TNF-α induced ROS elevation. In support of this notion, others have shown that increased necroptosis triggers ROS and inhibition of necroptosis reduces ROS in cultured cardiomyocytes [32]. Likewise, Nec-1 inhibits necroptosis and apoptosis in doxorubicin-induced cardiomyopathy characterized by excessive inflammatory cytokines and oxidative stress [32]. Nec-1 improves mitochondrial function, suppresses inflammation and reduces pro-apoptotic protein Bax and increases anti-apoptotic protein Bcl-2 expression in prediabetic rats [33]. Evidence has accumulated that TNF-α induces activation of NADPH oxidase, a major source of ROS [34], in human and animal cardiomyocytes [35,36].

GSK2795039 prevents TNF-α-induced Nox2 expression and ROS in cardiomyocytes

Our recent studies have demonstrated that GSK2795039, a novel small molecular Nox2 inhibitor [16,17], inhibits NADPH oxidase and oxidative stress in doxorubicin-induced cardiomyopathy [20,26], which is characterized by increased inflammatory cytokines [37,38]. In the present study, we have shown that GSK2795039 prevented TNF-α-induced increases in Nox2 protein expression and intracellular ROS in H9C2 cardiomyocytes. In support of our findings, other studies have shown that GSK2795039 inhibits Nox2-derived ROS production in an inflammation model [19]. Antioxidants attenuate proinflammatory cytokines, NADPH oxidase subunits and ROS in cardiomyopathy [39,40]. GKT137831, a dual inhibitor of both Nox1 and Nox4, attenuates proinflammatory cytokines such as TNF-α, IL-6 and IL-1β and oxidative stress in pressure overload-induced cardiac remodeling [41]. These data suggest that GSK2795039 prevents TNF-α-induced Nox2 expression and ROS in cardiomyocytes.

GSK2795039 prevents TNF-α-induced cardiomyocytes necroptosis

TNF-α has been shown to induce necroptosis in cardiomyocytes [12,13]. In the present study, we have shown that TNF-α increased protein expression of p-RIP1, p-RIP3 and p-MLKL, markers of necroptosis, in H9C2 cardiomyocytes. We have further demonstrated that the specific Nox2 inhibitor GSK2795039 prevented the increases in p-RIP1, p-RIP3 and p-MLKL protein expression in cardiomyocytes after exposure to TNF-α. In consistence with the present results, we recently demonstrated that GSK2795039 prevents necroptosis in cardiomyocytes after exposure to doxorubicin [20], which has been shown to induce TNF-α in cardiomyocytes [42]. Antioxidant N-acetylcysteine attenuates TNF-α, ROS and necroptosis in cardiomyocytes after exposure to high glucose [43]. Melatonin decreases TNF-α levels, reduces ROS and suppresses RIP3-MLKL signaling induced myocyte necroptosis in myocardial ischemia and reperfusion [44]. These findings suggest that the specific Nox2 inhibitor GSK2795039 prevents TNF-α-induced cardiomyocyte necroptosis through inhibition of RIP1-RIP3-MLKL signaling pathway.

GSK2795039 prevents TNF-α-induced cardiomyocyte apoptosis

Extensive research has demonstrated that TNF-α induces cardiomyocyte apoptosis [45]. Our present study has shown that TNF-α induced apoptosis assessed by an increase in cleaved caspase 3 protein expression, a marker of apoptosis, in H9C2 cardiomyocyte, the specific Nox2 inhibitor GSK2795039 prevented TNF-α-induced cardiomyocyte apoptosis. In agreement with the present findings, antioxidant N-acetylcysteine abrogates norepinephrine-induced TNF-α secretion, caspase activation, and apoptosis in neonatal rat cardiomyocytes [46]. Antioxidant phenolic acid protects cardiomyocytes from TNF-α-induced apoptosis [47]. These data suggest that the specific Nox2 inhibitor GSK2795039 prevents TNF-α-induced cardiomyocytes apoptosis.

Limitations

The present study focused primarily on the effects of the specific Nox2 inhibitor GSK2795039 on TNF-α-induced necroptosis in H9C2 cardiomyocytes. This study was not designed to determine the effects of GSK2795039 in neonatal or adult cardiomyocytes and *in vivo* models. Further studies are warranted to validate in primary cardiomyocytes and/or *in vivo* models of heart failure.

Conclusions

In the present study, we have demonstrated for

the first time that in H9C2 cardiomyocytes in culture, GSK2795039 inhibited TNF-α-induced Nox2 expression and intracellular ROS, prevented TNF-α-induced increases in p-RIP1, p-RIP3 and p-MLKL proteins, attenuated TNF-α-induced reduction in Bcl-2 protein and the increases in Bax protein, phosphorylated JNK protein and cleaved caspase 3 protein (Fig. 6E). These findings suggest that GSK2795039 prevents TNF-α-induced RIP1-RIP3-MLKL-mediated necroptosis in H9C2 cardiomyocytes through inhibition of NADPH oxidase-derived ROS. These observations could pave the way for the evaluation of GSK2795039 in experimental heart failure, which is characterized by excessive inflammatory cytokines such as TNF-α and oxidative stress.

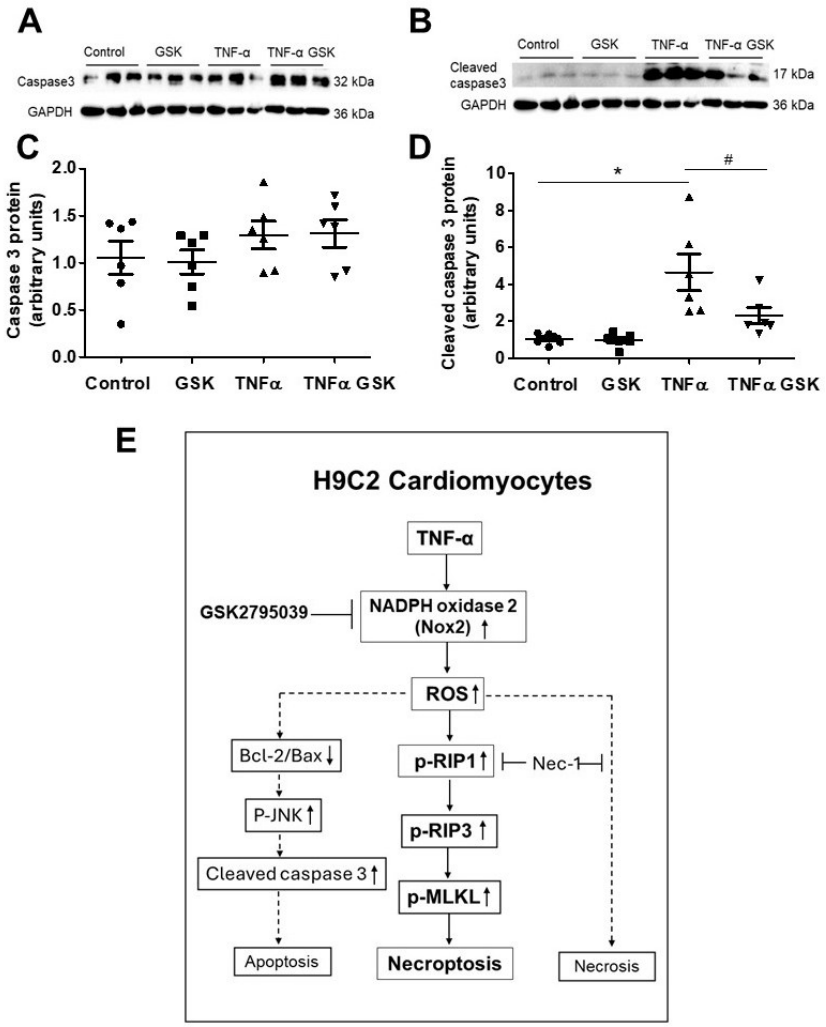


Fig. 6. (**A-D**) Effect of the Nox2 inhibitor GSK2795039 (GSK) on caspase 3 and cleaved caspase 3 protein expression in H9C2 cardiomyocytes after exposure to tumor necrosis factor-α (TNF-α). Representative Western blots of caspase 3 and cleaved caspase 3 proteins, respectively. Equal loading of proteins is illustrated by GAPDH bands. The graphs show the relative expression of caspase 3 and cleaved caspase 3 proteins in the four groups, respectively. Values are means ± S.D.; n=6. * P<0.05 vs. Control or GSK group; # P<0.05 vs. TNF-α group. (**E**) GSK2795039 inhibits the NADPH oxidase subunit gp91phox (Nox2) protein expression, reduces reactive oxygen species (ROS), prevents the increases in phosphorylated RIP1 (p-RIP1), p-RIP3 and p-MLKL proteins, reflective of their activities, markers of necroptosis, in H9C2 cardiomyocytes after exposure to tumor necrosis factor-α (TNF-α). GSK2795039 also arrests the decrease in Bcl-2/Bax ratio and the increases in p-JNK, reflective of JNK activity, and cleaved caspase 3, indicative of caspase activity, a marker of apoptosis, in H9C2 cardiomyocytes after exposure to TNF-α. The RIP1 inhibitor Nec-1 inhibits TNF-α-induced necrosis and necroptosis. GSK2795039 prevents TNF-α-induced RIP1-RIP3-MLKL-mediated cardiomyocyte necroptosis through inhibition of NADPH oxidase.

Conflict of Interest

There is no conflict of interest.

Acknowledgements

This work was supported by the National Natural Science Foundation of China (Grant numbers 81670369, 81870214, 82470409 to F.Z.Q).

References

1. Papamichail A, Kourek C, Briasoulis A, Xanthopoulos A, Tsougos E, Farmakis D, et al. Targeting Key Inflammatory Mechanisms Underlying Heart Failure: A Comprehensive Review. Int J Mol Sci 2023;25:510. https://doi.org/10.3390/ijms25010510
2. Joulin O, Petillot P, Labalette M, Lancel S, Neviere R. Cytokine profile of human septic shock serum inducing cardiomyocyte contractile dysfunction. Physiol Res 2007;56:291-297. https://doi.org/10.33549/physiolres.930946
3. Garofalo M, Corso R, Tomasoni D, Adamo M, Lombardi CM, Inciardi RM, et al. Inflammation in acute heart failure. Front Cardiovasc Med 2023;10:1235178. https://doi.org/10.3389/fcvm.2023.1235178
4. Zhang H, Dhalla NS. The Role of Pro-Inflammatory Cytokines in the Pathogenesis of Cardiovascular Disease. Int J Mol Sci 2024;25:1082. https://doi.org/10.3390/ijms25021082
5. Feldman AM, Combes A, Wagner D, Kadakomi T, Kubota T, Li YY, et al. The role of tumor necrosis factor in the pathophysiology of heart failure. J Am Coll Cardiol 2000;35:537-544. https://doi.org/10.1016/S0735-1097(99)00600-2
6. Arvunescu AM, Ionescu RF, Cretoiu SM, Dumitrescu SI, Zaharia O, Nanea IT. Inflammation in Heart Failure-Future Perspectives. J Clin Med 2023;12:7738. https://doi.org/10.3390/jcm12247738
7. Kubota T, McTiernan CF, Frye CS, Slawson SE, Lemster BH, Koretsky AP, et al. Dilated cardiomyopathy in transgenic mice with cardiac-specific overexpression of tumor necrosis factor-alpha. Circ Res 1997;81:627-635. https://doi.org/10.1161/01.RES.81.4.627
8. Yokoyama T, Nakano M, Bednarczyk JL, McIntyre BW, Entman M, Mann DL. Tumor necrosis factor-alpha provokes a hypertrophic growth response in adult cardiac myocytes. Circulation 1997;95:1247-1252. https://doi.org/10.1161/01.CIR.95.5.1247
9. Haudek SB, Taffet GE, Schneider MD, Mann DL. TNF provokes cardiomyocyte apoptosis and cardiac remodeling through activation of multiple cell death pathways. J Clin Invest 2007;117:2692-2701. https://doi.org/10.1172/JCI29134
10. Lichy M, Szobi A, Hrdlicka J, Horvath C, Kormanova V, Rajtik T, et al. Different signalling in infarcted and non-infarcted areas of rat failing hearts: A role of necroptosis and inflammation. J Cell Mol Med 2019;23:6429-6441. https://doi.org/10.1111/jcmm.14536
11. Adameova A, Goncalvesova E, Szobi A, Dhalla NS. Necroptotic cell death in failing heart: relevance and proposed mechanisms. Heart Fail Rev 2016;21:213-221. https://doi.org/10.1007/s10741-016-9537-8
12. Ogasawara M, Yano T, Tanno M, Abe K, Ishikawa S, Miki T, et al. Suppression of autophagic flux contributes to cardiomyocyte death by activation of necroptotic pathways. J Mol Cell Cardiol 2017;108:203-213. https://doi.org/10.1016/j.yjmcc.2017.06.008
13. Marunouchi T, Nishiumi C, Iinuma S, Yano E, Tanonaka K. Effects of Hsp90 inhibitor on the RIP1-RIP3-MLKL pathway during the development of heart failure in mice. Eur J Pharmacol 2021;898:173987. https://doi.org/10.1016/j.ejphar.2021.173987
14. Suematsu N, Tsutsui H, Wen J, Kang D, Ikeuchi M, Ide T, et al. Oxidative stress mediates tumor necrosis factor-alpha-induced mitochondrial DNA damage and dysfunction in cardiac myocytes. Circulation 2003;107:1418-1423. https://doi.org/10.1161/01.CIR.0000055318.09997.1F
15. Visnagri A, Oexner RR, Kmiotek-Wasylewska K, Zhang M, Zoccarato A, Shah AM. Nicotinamide Adenosine Dinucleotide Phosphate Oxidase-Mediated Signaling in Cardiac Remodeling. Antioxid Redox Signal 2023;38:371-387. https://doi.org/10.1089/ars.2022.0176
16. Liu J, Lu Y, Ping N, Li X, Lin Y, Li C. Apocynin ameliorates pressure overload-induced cardiac remodeling by inhibiting oxidative stress and apoptosis. Physiol Res 2017;66:741-752. https://doi.org/10.33549/physiolres.933257
17. Moe KT, Khairunnisa K, Yin NO, Chin-Dusting J, Wong P, Wong MC. Tumor necrosis factor-alpha-induced nuclear factor-kappaB activation in human cardiomyocytes is mediated by NADPH oxidase. J Physiol Biochem 2014;70:769-779. https://doi.org/10.1007/s13105-014-0345-0
18. Chocry M, Leloup L. The NADPH Oxidase Family and Its Inhibitors. Antioxid Redox Signal 2020;33:332-353. https://doi.org/10.1089/ars.2019.7915

19. Hirano K, Chen WS, Chueng ALW, Dunne AA, Seredenina T, Filippova A, et al. Discovery of GSK2795039, a Novel Small Molecule NADPH Oxidase 2 Inhibitor. Antioxid Redox Signal 2015;23:358-374. https://doi.org/10.1089/ars.2014.6202
20. Zhang X, Li L, Wang A, Guo H, Zhao H, Chi R, et al. GSK2795039 prevents RIP1-RIP3-MLKL-mediated cardiomyocyte necroptosis in doxorubicin-induced heart failure through inhibition of NADPH oxidase-derived oxidative stress. Toxicol Appl Pharmacol 2023;463:116412. https://doi.org/10.1016/j.taap.2023.116412
21. Al-Chlaihawi M, Janabi A. Azilsartan improves doxorubicin-induced cardiotoxicity via inhibiting oxidative stress, proinflammatory pathway, and apoptosis. J Med Life 2023;16:1783-1788. https://doi.org/10.25122/jml-2023-0106
22. Li B, Tian J, Sun Y, Xu T, Chi R, Zhang X, et al. Activation of NADPH oxidase mediates increased endoplasmic reticulum stress and left ventricular remodeling after myocardial infarction in rabbits. Biochim Biophys Acta 2015;1852:805-815. https://doi.org/10.1016/j.bbadis.2015.01.010
23. Abe K, Yano T, Tanno M, Miki T, Kuno A, Sato T, et al. mTORC1 inhibition attenuates necroptosis through RIP1 inhibition-mediated TFEB activation. Biochim Biophys Acta Mol Basis Dis 2019;1865:165552. https://doi.org/10.1016/j.bbadis.2019.165552
24. Ogasawara M, Yano T, Tanno M, Abe K, Ishikawa S, Miki T, et al. Suppression of autophagic flux contributes to cardiomyocyte death by activation of necroptotic pathways. J Mol Cell Cardiol 2017;108:203-213. https://doi.org/10.1016/j.yjmcc.2017.06.008
25. Marunouchi T, Nishiumi C, Iinuma S, Yano E, Tanonaka K. Effects of Hsp90 inhibitor on the RIP1-RIP3-MLKL pathway during the development of heart failure in mice. Eur J Pharmacol 2021;898:173987. https://doi.org/10.1016/j.ejphar.2021.173987
26. Zhao H, Ma Y, Zhang X, Guo H, Yang B, Chi R, et al. NADPH oxidase 2 inhibitor GSK2795039 prevents doxorubicin-induced cardiac atrophy by attenuating cardiac sympathetic nerve terminal abnormalities and myocyte autophagy. Eur J Pharmacol 2024;967:176351. https://doi.org/10.1016/j.ejphar.2024.176351
27. Szobi A, Goncalvesova E, Varga ZV, Leszek P, Kusmierczyk M, Hulman M, et al. Analysis of necroptotic proteins in failing human hearts. J Transl Med 2017;15:86-85. https://doi.org/10.1186/s12967-017-1189-5
28. Engel D, Peshock R, Armstong RC, Sivasubramanian N, Mann DL. Cardiac myocyte apoptosis provokes adverse cardiac remodeling in transgenic mice with targeted TNF overexpression. Am J Physiol Heart Circ Physiol 2004;287:1303. https://doi.org/10.1152/ajpheart.00053.2004
29. Cebova M, Barta A, Bujnova K, Vojtkova M, Vrankova S, Klimentova J, et al. Modulation of Cardiac Gene Expression by anti-HMGB1 in a Model of Experimental Myocardial Infarction. Physiol Res 2025;74(Suppl 2):S259-S269. https://doi.org/10.33549/physiolres.935718
30. Adameova A, Horvath C, Abdul-Ghani S, Varga ZV, Suleiman MS, Dhalla NS. Interplay of Oxidative Stress and Necrosis-like Cell Death in Cardiac Ischemia/Reperfusion Injury: A Focus on Necroptosis. Biomedicines 2022;10:127. https://doi.org/10.3390/biomedicines10010127
31. Chi R, Li L, Wang A, Yang H, Xi J, Zhu Z, et al. Enhanced oxidative stress mediates pathological autophagy and necroptosis in cardiac myocytes in pressure overload induced heart failure in rats. Clin Exp Pharmacol Physiol 2022;49:60-69. https://doi.org/10.1111/1440-1681.13583
32. Erdogmus Ozgen Z, Erdinc M, Kelle I, Erdinc L, Nergiz Y. Protective effects of necrostatin-1 on doxorubicin-induced cardiotoxicity in rat heart. Hum Exp Toxicol 2022;41:9603271211066066. https://doi.org/10.1177/09603271211066066
33. Apaijai N, Jinawong K, Singhanat K, Jaiwongkam T, Kerdphoo S, Chattipakorn SC, et al. Necrostatin-1 reduces cardiac and mitochondrial dysfunction in prediabetic rats. J Endocrinol 2021;251:27-39. https://doi.org/10.1530/JOE-21-0134
34. Visnagri A, Oexner RR, Kmiotek-Wasylewska K, Zhang M, Zoccarato A, Shah AM. Nicotinamide Adenosine Dinucleotide Phosphate Oxidase-Mediated Signaling in Cardiac Remodeling. Antioxid Redox Signal 2023;38:371-387. https://doi.org/10.1089/ars.2022.0176
35. Moe KT, Khairunnisa K, Yin NO, Chin-Dusting J, Wong P, Wong MC. Tumor necrosis factor-alpha-induced nuclear factor-kappaB activation in human cardiomyocytes is mediated by NADPH oxidase. J Physiol Biochem 2014;70:769-779. https://doi.org/10.1007/s13105-014-0345-0

36. Moe KT, Yin NO, Naylynn TM, Khairunnisa K, Wutyi MA, Gu Y, et al. Nox2 and Nox4 mediate tumour necrosis factor-alpha-induced ventricular remodelling in mice. J Cell Mol Med 2011;15:2601-2613. https://doi.org/10.1111/j.1582-4934.2011.01261.x
37. Quagliariello V, Canale ML, Bisceglia I, Iovine M, Paccone A, Maurea C, et al. Sodium-glucose cotransporter 2 inhibitor dapagliflozin prevents ejection fraction reduction, reduces myocardial and renal NF-kappaB expression and systemic pro-inflammatory biomarkers in models of short-term doxorubicin cardiotoxicity. Front Cardiovasc Med 2024;11:1289663. https://doi.org/10.3389/fcvm.2024.1289663
38. Al-Chlaihawi M, Janabi A. Azilsartan improves doxorubicin-induced cardiotoxicity via inhibiting oxidative stress, proinflammatory pathway, and apoptosis. J Med Life 2023;16:1783-1788. https://doi.org/10.25122/jml-2023-0106
39. Thandavarayan RA, Giridharan VV, Arumugam S, Suzuki K, Ko KM, Krishnamurthy P, et al. Schisandrin B prevents doxorubicin induced cardiac dysfunction by modulation of DNA damage, oxidative stress and inflammation through inhibition of MAPK/p53 signaling. PLoS One 2015;10:e0119214. https://doi.org/10.1371/journal.pone.0119214
40. Fang G, Li X, Yang F, Huang T, Qiu C, Peng K, et al. Galangin attenuates doxorubicin-induced cardiotoxicity via activating nuclear factor erythroid 2-related factor 2/heme oxygenase 1 signaling pathway to suppress oxidative stress and inflammation. Phytother Res 2023;37:5854-5870. https://doi.org/10.1002/ptr.7991
41. Zeng S, Yang L, Yan Q, Gao L, Lu H, Yan P. Nox1/4 dual inhibitor GKT137831 attenuates hypertensive cardiac remodelling associating with the inhibition of ADAM17-dependent proinflammatory cytokines-induced signalling pathways in the rats with abdominal artery constriction. Biomed Pharmacother 2019;109:1907-1914. https://doi.org/10.1016/j.biopha.2018.11.077
42. Jiang Y, Zhang Q. Catalpol ameliorates doxorubicin-induced inflammation and oxidative stress in H9C2 cells through PPAR-gamma activation. Exp Ther Med 2020;20:1003-1011. https://doi.org/10.3892/etm.2020.8743
43. Liang W, Chen M, Zheng D, He J, Song M, Mo L, et al. A novel damage mechanism: Contribution of the interaction between necroptosis and ROS to high glucose-induced injury and inflammation in H9c2 cardiac cells. Int J Mol Med 2017;40:201-208. https://doi.org/10.3892/ijmm.2017.3006
44. Yang Z, Li C, Wang Y, Yang J, Yin Y, Liu M, et al. Melatonin attenuates chronic pain related myocardial ischemic susceptibility through inhibiting RIP3-MLKL/CaMKII dependent necroptosis. J Mol Cell Cardiol 2018;125:185-194. https://doi.org/10.1016/j.yjmcc.2018.10.018
45. Engel D, Peshock R, Armstong RC, Sivasubramanian N, Mann DL. Cardiac myocyte apoptosis provokes adverse cardiac remodeling in transgenic mice with targeted TNF overexpression. Am J Physiol Heart Circ Physiol 2004;287:H1303-H1311. https://doi.org/10.1152/ajpheart.00053.2004
46. Fu Y, Chi C, Yin S, Hwang B, Chiu Y, Hsu S. Norepinephrine induces apoptosis in neonatal rat cardiomyocytes through a reactive oxygen species-TNF alpha-caspase signaling pathway. Cardiovasc Res 2004;62:558-567. https://doi.org/10.1016/j.cardiores.2004.01.039
47. Li C, Chen L, Song M, Fang Z, Zhang L, Coffie JW, et al. Ferulic acid protects cardiomyocytes from TNF-alpha/cycloheximide-induced apoptosis by regulating autophagy. Arch Pharm Res 2020;43:863-784. https://doi.org/10.1007/s12272-020-01252-z